Physica Medica 66 (2019) 66–76

Contents lists available at ScienceDirect

Physica Medica

journal homepage: www.elsevier.com/locate/ejmp

BrachyView: Reconstruction of seed positions and volume of an LDR prostate brachytherapy patient plan using a baseline subtraction algorithm

T. Brennen[a,*], D.L. Cutajar[a,b], S. Alnaghy[a], J. Bucci[a], A. Bece[b], K. Enari[b], M. Favoino[c], F. Carriero[c], M. Tartaglia[c], L. Galli[c], M. Lerch[a], A.B. Rosenfeld[a], M. Petasecca[a]

[a] Centre for Medical Radiation Physics, University of Wollongong, Wollongong, New South Wales, Australia
[b] St George Cancer Care Centre, St George Hospital, Kogarah, New South Wales, Australia
[c] Exprivia SpA, Molfetta, Italy

ARTICLE INFO

Keywords:
Brachytherapy
Baseline subtraction
Intraoperative dosimetry
Prostate

ABSTRACT

Purpose: BrachyView is a novel in-body imaging system developed with the objective to provide real-time intraoperative dosimetry for low dose rate (LDR) prostate brachytherapy treatments. The BrachyView coordinates combined with conventional transrectal ultrasound (TRUS) imaging, provides the possibility to localise the effective position of the implanted seeds inside the prostate volume, providing a unique tool for intra-operative verification of the quality of the implantation. This research presents the first complete LDR brachytherapy plan reconstructed by the BrachyView system and is used to evaluate the effectiveness of an imaging algorithm with baseline subtraction.

Methods: A plan featuring 98 I-125 brachytherapy seeds, with an average activity of 0.248 mCi, were implanted into a prostate gel phantom under TRUS guidance. Images of implanted seeds were obtained by the BrachyView after the implantation of seeds. The baseline subtraction algorithm is applied as a pixel-to-pixel counts subtraction and is applied to every second projection obtained after the implantation of each needle. Seed positions and effectiveness of the baseline reconstruction in the identification of seeds were verified by a high-resolution post-implant CT scan.

Results: A complete brachytherapy plan has been reconstructed with a 100% detection rate. This is possible due to the effectiveness of the baseline subtraction, with its application an overall increase of 11.3% in position accuracy and 8.2% increase in detection rate was noted.

Conclusion: It has been demonstrated that the BrachyView system shows the potential to be a solution to providing clinics with the means for intraoperative dosimetry for LDR prostate brachytherapy treatments.

1. Introduction

In 2017, prostate cancer was the most commonly diagnosed cancer, accounting for approximately 25% of cancer treatments in Australia [1]. Low dose rate (LDR) brachytherapy is a common treatment option for cancer of the prostate due to its slow proliferating nature and highly precise conformal dose delivery under direct visualisation [2]. With advancements in treatments, it is becoming ever critical to minimise the dose that may be delivered to surrounding healthy tissues during treatments. In LDR treatments, this undesirable dose may result from seed positioning errors. Seed displacement can be caused by a number of factors including prostate motion and deformation [3,4], needle bending [5,6] and prostate swelling [7]. The effects of seed placement deviations from pre-planned positions in ultrasound guided prostate implants have been previously investigated by Dawson et al. in a simulation planning study with 48 I-125 brachytherapy seeds, and a dose prescription of 160 Gy to the reference distance [8]. Results showed that with a deviation from the planned treatment position as small as 2mm, cold spots (underdose) of 8% and hot spots (overdose) of 12% resulted. These results demonstrate the necessity to identify errors in seed positioning which modify the dose distributions from those planned, which compromise the treatment outcomes [9].

1.1. Current seed reconstruction methodologies

Currently, there are two main imaging modalities implemented in seed position verification during treatment and for post-operative dosimetry verification for LDR brachytherapy. These are transrectal

* Corresponding author.
E-mail address: tjb790@uowmail.edu.au (T. Brennen).

https://doi.org/10.1016/j.ejmp.2019.09.237
Received 9 April 2019; Received in revised form 13 September 2019; Accepted 19 September 2019
Available online 26 September 2019
1120-1797/ © 2019 Associazione Italiana di Fisica Medica. Published by Elsevier Ltd. All rights reserved.

ultrasound (TRUS) guidance and C-arm fluoroscopy imaging. TRUS guidance is utilised during implantation to visualise the prostate and surrounding anatomy to guide the insertion of needles containing the brachytherapy seeds. TRUS imaging provides visualisation of soft tissue, making it ideal for prostate visualisation, however, due to the limited spatial resolution of ultrasound transceivers the identification of implanted seeds is often impossible due to the low echogenic nature of the metallic implanted seeds [10].

TRUS imaging can also be coupled with fluoroscopy imaging, where mobile C-arms can deliver a continuous X-ray beam at a range of angles for dynamic imaging during the procedure. Utilising a limited projection method, 3D reconstruction of the volume and implanted seeds can be obtained and co-registered to TRUS images [11]. The current practice for seed localisation utilises co-registration of one or two fluoroscopic images from a C-arm unit and soft tissue imaging from TRUS. However, segmentation with this technology is only accurate for seeds that are visible and can result in some seeds being undefined due to overlapping with other seeds, which has been shown to occur in up to 26% of seeds [12]. Algorithms have been developed to aid in solving the “hidden seed problem”, however, their performance degrades as the number of hidden seeds increases [13]. Errors as large as 3 mm can occur due to registration errors between the TRUS and fluoroscopy images resulting from artefacts present on TRUS images being mistaken for brachytherapy seeds, introducing dosimetric uncertainty [10]. Clinics have reported hidden seeds that have not been identified by co-registered TRUS and fluoroscopic images ranging between 7% and 45% [10].

Real-time intraoperative CT assessment of prostate seed implantation was investigated by Zelefsky et al., using cone beam computerised tomography (CBCT) to extract seed coordinate data [14,15]. This allowed for assessment of the dose coverage to the prostate with seed implantation, however, the method required three separate CBCT images, two directly following the implantation of all the seeds and a final image obtained approximately 3 h post operation. Changes in dose coverage caused by suboptimal implantations were detectable, however, this method requires a CBCT to be available in the operation theatre, additional scans with associated additional dose, and increased treatment times.

Another recent development is real-time electromagnetic seed drop detection for permanent brachytherapy implants, as developed by Philips [16]. The proposed system utilises a hollow needle sensor (for LDR) or stylet (for high dose rate (HDR)), where conventional tracking and seed detection is performed by monitoring the induced voltage between the two end terminals of the sensor coil. This can then be used to determine the localised 3D position of the seed within the prostate. 3D average and maximum drop errors, when compared to optically assessed positions, were $0.6^{+1.2}_{-0.5}$ mm and $2.1^{+1.1}_{-0.8}$ mm [16], respectively. EM tracking has also been fused with TRUS imaging to achieve seed localisation. Seed drop locations are recorded by the EM sensors and used to detect the false positives located in the conventional TRUS-based seed detection method, as well as to estimate the positions of missing seeds. EM-only seed detection was able to achieve a localisation mean error of 3.7 mm with a detection rate of 100%, but when fused with TRUS imaging, a mean error of 1.8 mm was achieved while maintaining a 100% detection rate [17]. Though this methodology produced a 100% detection rate for four types of brachytherapy seeds, implementation may be costly for centres to employ as each needle for LDR treatments must contain an EM sensor, or if a single hollow EM needle is utilised, a substantial amount of time would be required to perform needle loading during implantation.

1.2. The BrachyView system

As the requirement to minimise suboptimal brachytherapy implantations increases, a method for effective real-time intraoperative dosimetry is still required. Post-operative dosimetry is commonly assessed between 3 and 4 weeks post-implantation and can predict toxicity, identify undesirable cold spots and anticipate late effects developed by the patient. Without the possibility to modify or improve the implant, little can be done to rectify any misplacement [11,18], resulting in some patients requiring another brachytherapy treatment to deposit additional seeds to correct cold spots or supplemental external beam radiation therapy [19].

For intraoperative dosimetric verification for prostate LDR brachytherapy we propose BrachyView. The principle of operation of the BrachyView system has been previously published [20] and in summary, offers an in-body imaging system that provides real-time intraoperative localisation by reconstructing LDR seed positions in 3D directly after their implantation, by the means of a high-resolution pinhole gamma camera. Prior studies have demonstrated reconstruction of 30 active (0.400–0.418 mCi) I-125 brachytherapy seeds with 75% of seeds within 1 mm of their nominal positions [21–23,20]. Hardware optimisation of the system has also been completed, establishing that the use of an 800 μm collimator for reconstruction of seeds before their deployment from needles is not appropriate at this stage as

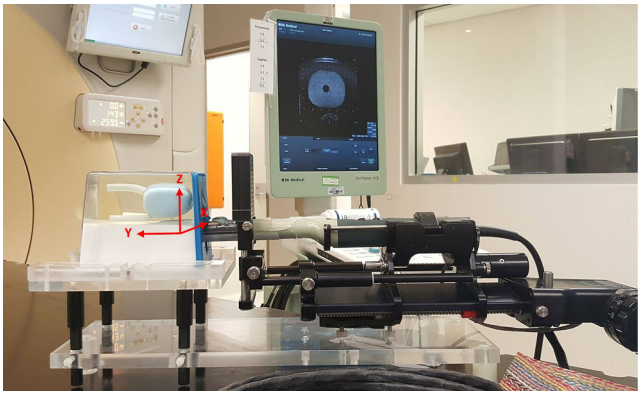

Fig. 1. Experimental configuration- the TRUS probe is inserted into the CIRS prostate gel phantom and is mounted onto the PMMA stand. The BrachyView coordinate frame utilised for reconstruction is also shown.

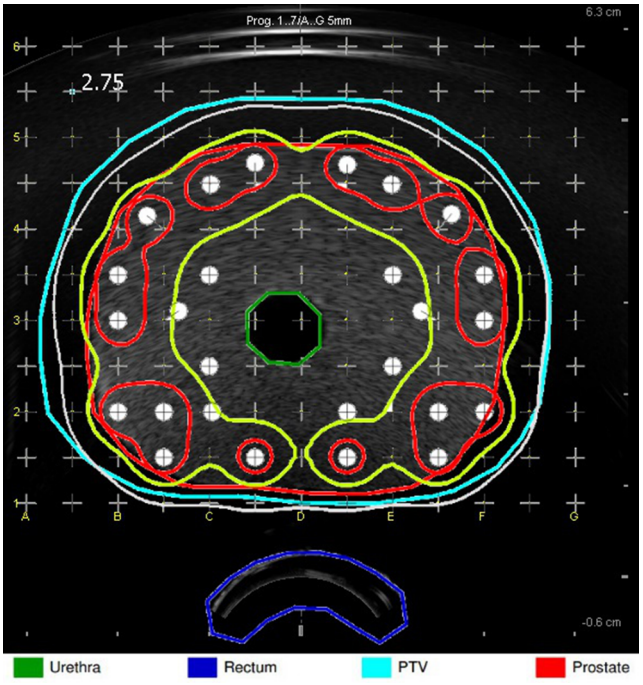

Fig. 2. Identification of the OARs (rectum and urethra), PTV and prostate margins overlaid on the TRUS image for the corresponding slice (2.75 cm).

a)

Needle Number	Retraction (cm)	Hole Location	Number Seeds
1	0.50	C4.5	5
2	0.00	c4.5	5
3	0.00	d4.5	5
4	0.50	E4.5	5
5	0.00	b4.0	5
6	0.00	e4.0	5
7	0.50	B3.5	5
8	*0.00*	*C3.5*	*2*
9	*0.00*	*E3.5*	*2*
10	0.50	F3.5	5
11	0.00	B3.0	5
12	*-0.50*	*b3.0*	*2*
13	*-0.50*	*e3.0*	*2*
14	0.00	F3.0	5
15	*0.00*	*C2.5*	*2*
16	*0.00*	*E2.5*	*2*
17	0.50	B2.0	4
18	*0.00*	*b2.0*	*4*
19	*-0.50*	*C2.0*	*2*
20	*-0.50*	*d2.0*	*2*
21	*0.00*	*e2.0*	*4*
22	0.50	F2.0	4
23	*1.00*	*b1.5*	*3*
24	0.00	c1.5	5
25	0.00	d1.5	5
26	*1.00*	*e1.5*	*3*

= Special loading

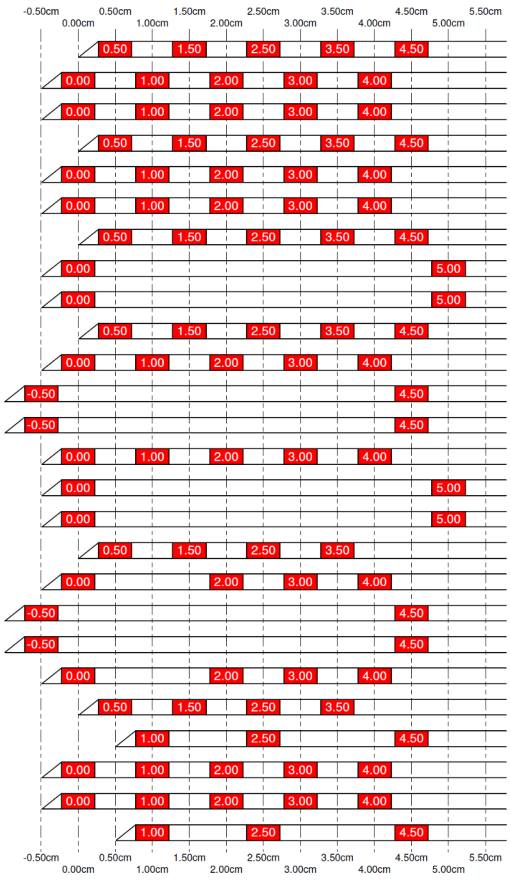

b)

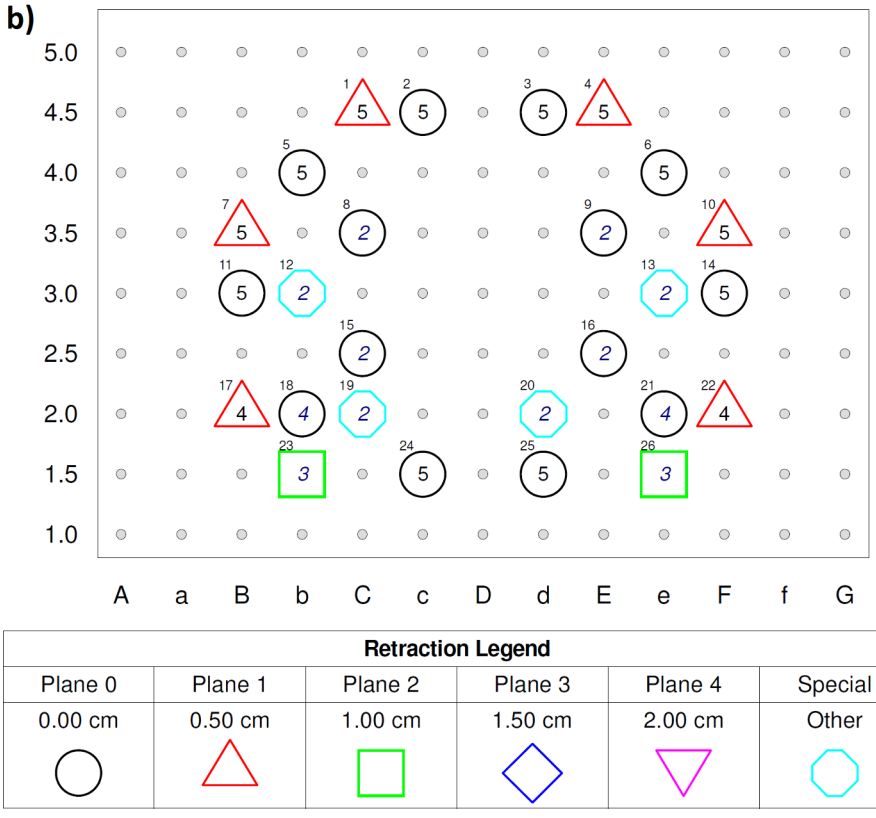

Retraction Legend					
Plane 0	Plane 1	Plane 2	Plane 3	Plane 4	Special
0.00 cm	0.50 cm	1.00 cm	1.50 cm	2.00 cm	Other

Fig. 3. VariSeed LDR brachytherapy treatment plan, a) needle loading table, depicting the planned seed locations within each needle, b) 2D needle grid pattern with plane locations for each needle tip.

Fig. 4. BrachyView probe wrapped in 70 μm Kapton tape prior to insertion into the gel phantom.

a great decrease in reconstruction accuracy and detection rate is noted [24]. The study presented in this work explores the capability of BrachyView in handling a clinically relevant number of seeds and examines how the number of seeds affects the amount of background radiation generated by the seeds themselves to quantify the background noise threshold, above which a seed's signal can be detected.

This study also presents the first full LDR brachytherapy plan implanted into a prostate gel phantom reconstructed in 3D and co-registered to the positions of the seeds for accurate evaluation of the clinical dose parameters.

2. Materials and methods

The US tissue-equivalent prostate gel phantom 053-I (CIRS Inc – Virginia US) [25] was utilised to assess the capabilities of the BrachyView system to deal with the reconstruction of an entire patient dataset.

To align and rigidly anchor the phantom and the TRUS probe, a custom polymethyl-methacrylate (PMMA) stand was used to attach the TRUS stepper unit used for ultrasound guidance during needle implantation, as shown in Fig. 1.

Cross-plane images of the prostate were acquired with the TRUS to produce a dataset for the reconstruction of the prostate volume. The base of the prostate was located, acting as the origin for the TRUS system, and subsequently used for the calculation of the treatment plan. A 5 mm margin was added to the prostate base along the superior-inferior axis (negative y-axis) to ensure complete coverage of the prostate volume. Images of the prostate were acquired with 2.5 mm increments. VariSeed (Varian Medical Systems, Inc – CA, US) was utilised for the calculation of the plan. Plan checking was conducted by a qualified medical physicist and radiation oncologist. The PTV, prostate, rectum and urethra were delineated by the oncologist, as shown in Fig. 2.

Twenty-six needles containing a total of 98 I-125 seeds, with an average source strength of 0.248 mCi were inserted into the prostate phantom using ultrasound guidance. Fig. 3 shows the treatment plan and needle arrangement of the procedure.

Needle implantation was performed based on AAPM TG-64 protocol [26]. The technique involved starting the first implant at the top left of the template and performing a raster scan to the bottom right. This methodology is favourable for BrachyView as it allows for the acquisition of images of distant seeds before they are masked by the seeds in closer proximity to the detector. After the deployment of all seeds within the needle, the TRUS probe was removed from the phantom cavity and replaced with the BrachyView probe. Each needle was individually imaged using a pixel by pixel baseline subtraction algorithm requiring the probe to maintain its position reproducibly for each captured image. The probe was realigned to the same position within the phantom for each insertion of the probe. This was performed using markers placed on the probe and phantom. The probe collimator consists of three single cone apertures of approximately 500 μm in diameter drilled into a 1 mm thick tungsten tube [21,23,20]. The probe was wrapped with 70 μm Kapton tape to reduce additional dose to the rectal wall due to backscattering [22] and prevent gel and liquid infiltrating the collimator through the pinholes, as shown in Fig. 4. An acquisition time of three minutes was used to account for the low activity of the seeds. A postoperative CT scan (Brilliance Big Bore, Philips, Andover, USA) of the phantom was carried out with the BrachyView probe in situ.The scan was performed with 1 mm slice thickness and 0.5 mm overlap with orthopedic metallic artifact reduction (OMAR) applied. The average total 3D discrepancy between the BrachyView data and CT data was calculated using Eqs. (1) and (2).

$$\sigma_{3D} = \sqrt{\sigma_x^2 + \sigma_y^2 + \sigma_z^2} \tag{1}$$

where:

$$\sigma_x = |X_{BV} - X_{CT}|, \quad \sigma_y = |Y_{BV} - Y_{CT}|, \quad \sigma_z = |Z_{BV} - Z_{CT}| \tag{2}$$

Two rigid-body registrations, guided by the PMMA stand and the urethra, were applied to register the BrachyView and CT images, seed positions and prostate anatomy to the same coordinate space. A 3D visualisation of seed positions (CT and BrachyView) contained within a 3D reconstruction of the implanted prostate volume was then produced with the TRUS slices obtained for the treatment planning system (TPS) [20].

The reconstruction methodology involves identification of the projections for each seed through each pinhole, and determining their

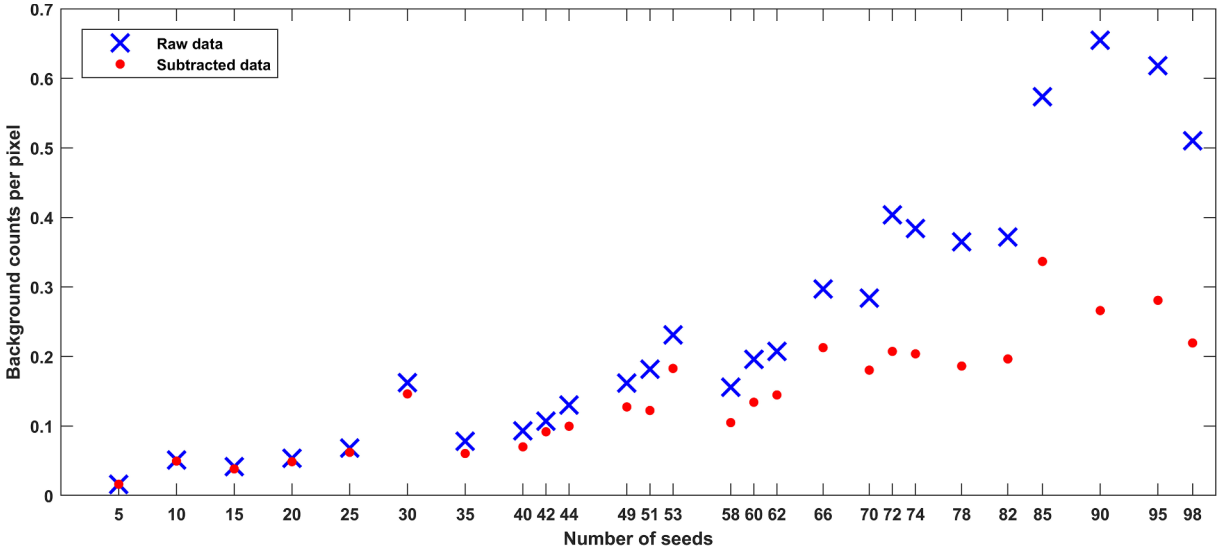

Fig. 5. Analysis of the baseline subtraction algorithms efficiency with an increasing number of brachytherapy sources implanted.

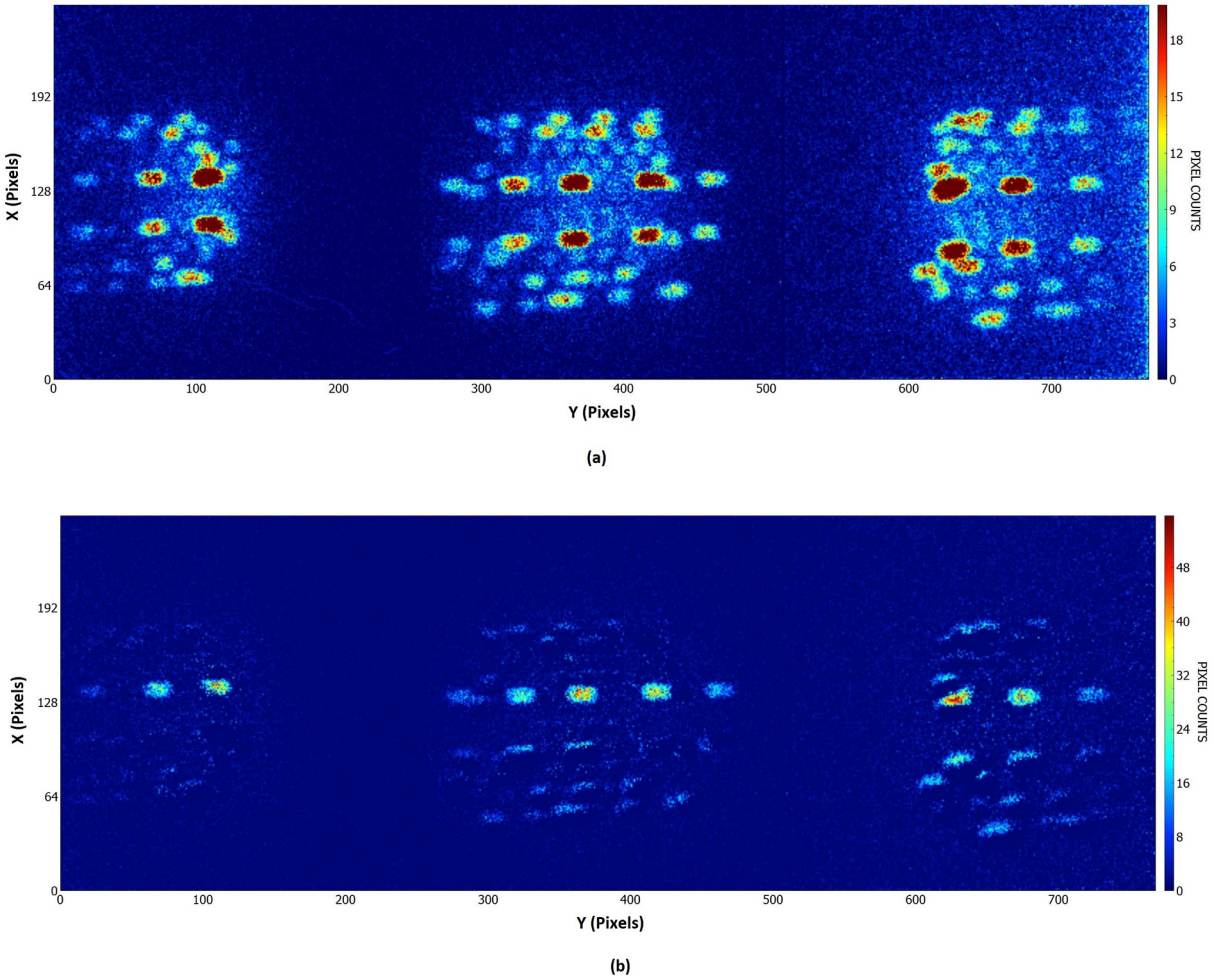

Fig. 6. (a) projections from 90 I-125 brachytherapy sources, (b) frame after application of the baseline subtraction algorithm, allowing for isolation of five newly inserted seeds for reconstruction.

center of mass (CoM) coordinates. Once the CoM coordinates are identified they are back projected through the relevant pinholes (known geometry of the BrachyView probe [20]) and a triangulation reconstruction method is implemented. With vector lines back projected through the relevant pinholes the 3D position of the seeds is given by the smallest distance between all vector lines. The probe was designed such that a minimum of two projections on the imaging plane is achievable at all times, given the probes field of view (FoV), providing the minimum number of vector lines required for the 3D reconstruction method [21,23,20].

A baseline subtraction method was applied to reconstruct the seeds within each needle to remove previously inserted seeds from the images. To avoid erroneous image subtractions caused by variations in the BrachyView probe position between image acquisition, each pair of current and previous images were aligned using a seed which was identified as the same seed in each image. Once alignment was performed, the background subtraction and imaging processing techniques [20] were then performed to optimise the reconstruction outcome.

The average number of background counts per pixel were analysed across a 40×795 pixel array representing an area across all acquired images. This technique was applied to images before and after the application of the baseline subtraction algorithm to assess how the background present within the images changes with an increasing number of seeds.

Dosimetric changes between the CT and BrachyView datasets were assessed by comparing the D90 and V100, from the VariSeed TPS. This was completed using the CT and BrachyView determined positions to generate cumulative dose volume histograms (DVH) for the prostate, planned treatment volume (PTV) and critical organs.

The procedure was consistent with the clinical workflow for LDR prostate treatments at our centre (St George Cancer Care Centre, NSW, Australia) to enable the assessment of the accuracy of the system in a clinical treatment scenario.

The above mentioned procedure was completed twice for the single set of obtained images. Once with baseline subtraction applied and once without. This allowed for the efficiency of the baseline subtraction algorithm to be assessed through comparison of detection rates, reconstruction accuracy, presence of scatter and variation in DVH and dose parameters for both cases.

3. Results

Fig. 5 compares the raw data and the data after the baseline subtraction algorithm was applied. Fig. 6 shows a frame acquired with the BrachyView system for all 90 I-125 seeds represented by the projections of the radiation emitted by each seed through the pinhole collimator. Insertion of the subsequent needle resulted in the presence of an additional five seeds. When the baseline subtraction algorithm was applied, the projections from the newly implanted seeds were identifiable allowing for easy identification and reconstruction. A detection rate of 91.8% was found for data without baseline subtraction applied, with the application of the baseline subtraction algorithm this was improved to give a detection rate of 100%.

The reconstructed seed positions from the BrachyView probe are

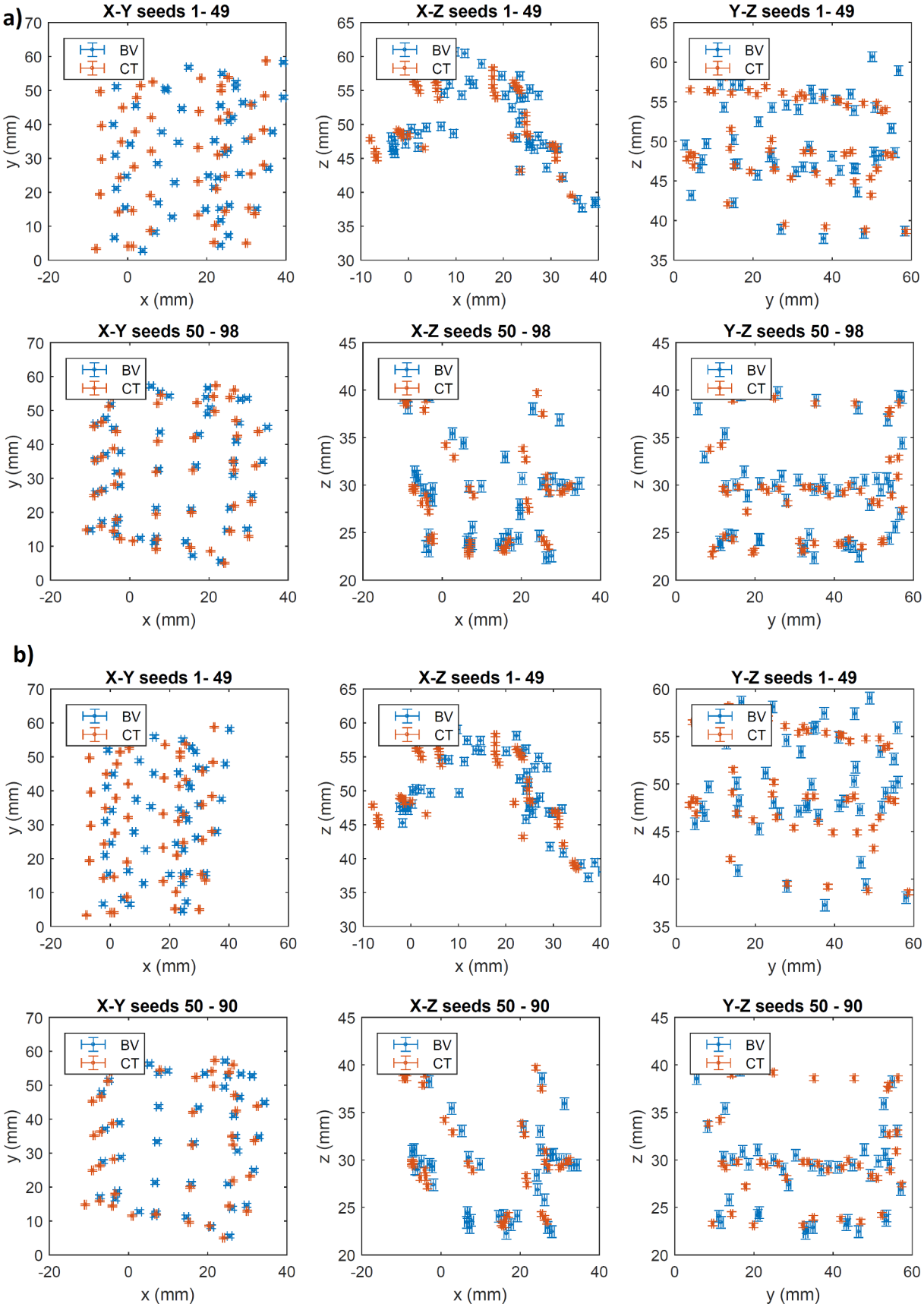

Fig. 7. 2D scatter plots of the BrachyView (blue) reconstructed positions and CT (orange) positions for a) baseline subtracted data and b) data processed without baseline subtraction. Errors were calculated based on CT resolution and the accuracy of the user determining a seeds' CoM. (For interpretation of the references to colour in this figure legend, the reader is referred to the web version of this article.)

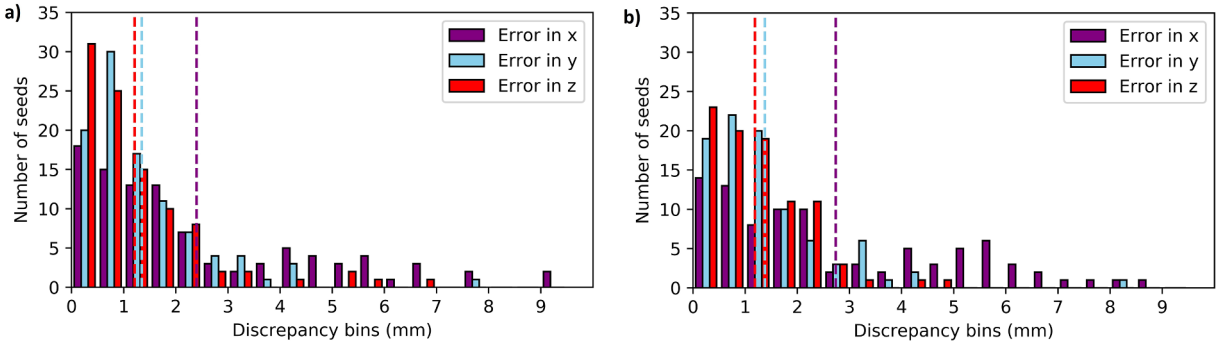

Fig. 8. Discrepancies between BrachyView reconstructed positions and post-implantation CT dataset, for x,y and z reference frames (dashed lines represent the average in the respective reference frame) for a) baseline subtracted data and b) data processed without baseline subtraction.

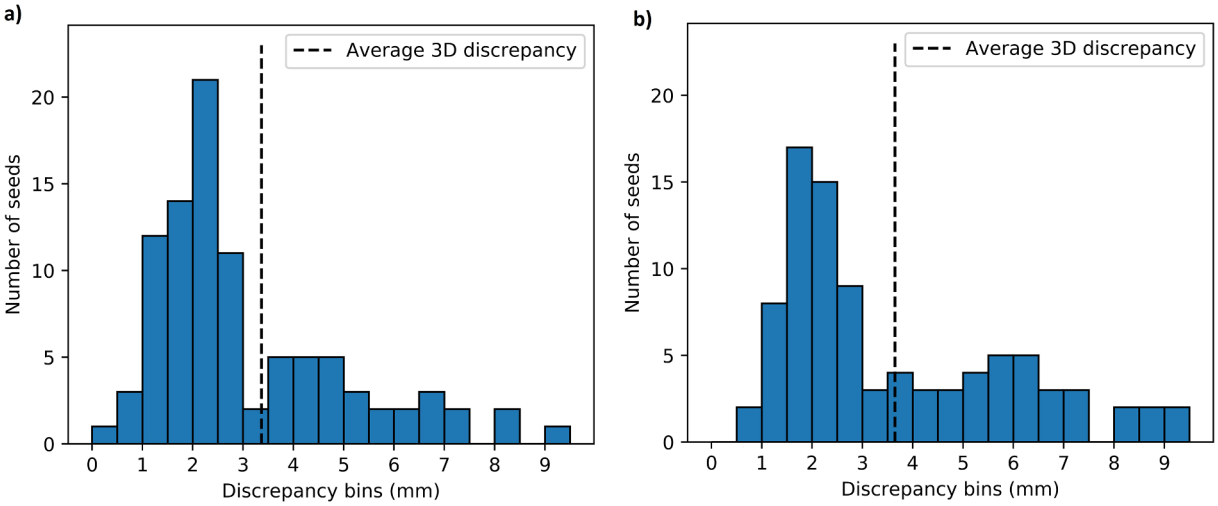

Fig. 9. Total 3D discrepancies between BrachyView reconstructed positions and post-implantation CT data set (dashed line represents the average 3D discrepancy) for a) baseline subtracted data and b) data without baseline subtraction.

shown in Fig. 7. Fig. 8 depicts the discrepancy between the BrachyView reconstructed positions and the CT determined positions in the x, y and z reference frames. Average discrepancies between BrachyView positions and the obtained CT dataset for baseline subtracted data where found to be 2.40 mm, 1.35 mm and 1.21 mm in the x, y and z reference frames, respectively. Approximately 69% of seeds were reconstructed within 2 mm of their nominal CT determined locations. The average total 3D discrepancy between the BrachyView data and CT data was found to be 3.28 mm, as shown in Fig. 9. For data without background subtraction applied average discrepancies were found to be 2.74 mm, 1.38 mm and 1.19 mm in the x, y and z reference frames, respectively. The average total discrepancy was found to be 3.65 mm, a decrease of 11.5% in reconstructed position (compared to the CT positions) when compared to data with baseline subtraction applied.

Fig. 10 shows the cumulative DVH (CDVH) calculated by the VariSeed TPS. Table 1 shows the calculated percentage difference between points of interest in the DVH values for the PTV, prostate, rectum and urethra. With Table 2 presenting the percentage differences for BrachyView data without baseline subtraction applied. Much larger discrepancies arise when comparing the organs at risk, such as the urethra with overestimations of dose as high as 185%. It was noted that without the application of the baseline subtraction algorithm this resulted in a decrease of 7.6% and 2.1% for D90 and V100 values, respectively, when compared to data obtained with baseline subtraction applied. Increased discrepancies between the PTV, prostate and rectum CDVH values when compared to those calculated with CT determined positions are also present.

A 3D reconstruction of the implanted prostate volume containing the seed positions (with baseline subtracted applied) for BrachyView (blue) and CT (red) is shown in Fig. 11. From inspection of the TRUS 3D reconstruction anatomical structures of the phantom such as the prostate volume, urethra and seminal vesicles are clearly identifiable, providing the user with clear visual information to aid in the assessment of the implantation quality.

4. Discussion

A major focus of this study was to assess the performance of the baseline subtraction algorithm using a full clinical plan. Implementation of the baseline subtraction algorithm produced a maximum reduction of 59.4% in background counts per pixel, greatly increasing the signal to noise ratio (SNR) for each newly implanted seed, as shown in Fig. 5. An interesting observation was a less than 2% variation in raw and baseline subtracted images when the number of seeds was fewer than 30. This was attributed to the low number of background counts and scatter present within these images. A minimum threshold of the number of seeds implanted before applying a baseline subtraction algorithm to the raw data would allow for the simplification of the image processing prior to reconstruction, reducing the computational load and timing for in vivo and real-time implant quality assessment.

Larger variations between measured and expected seed positions were observed in the study compared with previous work [20]. The errors predominantly occurred in the x-axis direction (left to right lateral anatomical direction) and are attributed to a rotation of the pinhole collimator of the BrachyView probe around the y-axis (inferior-superior

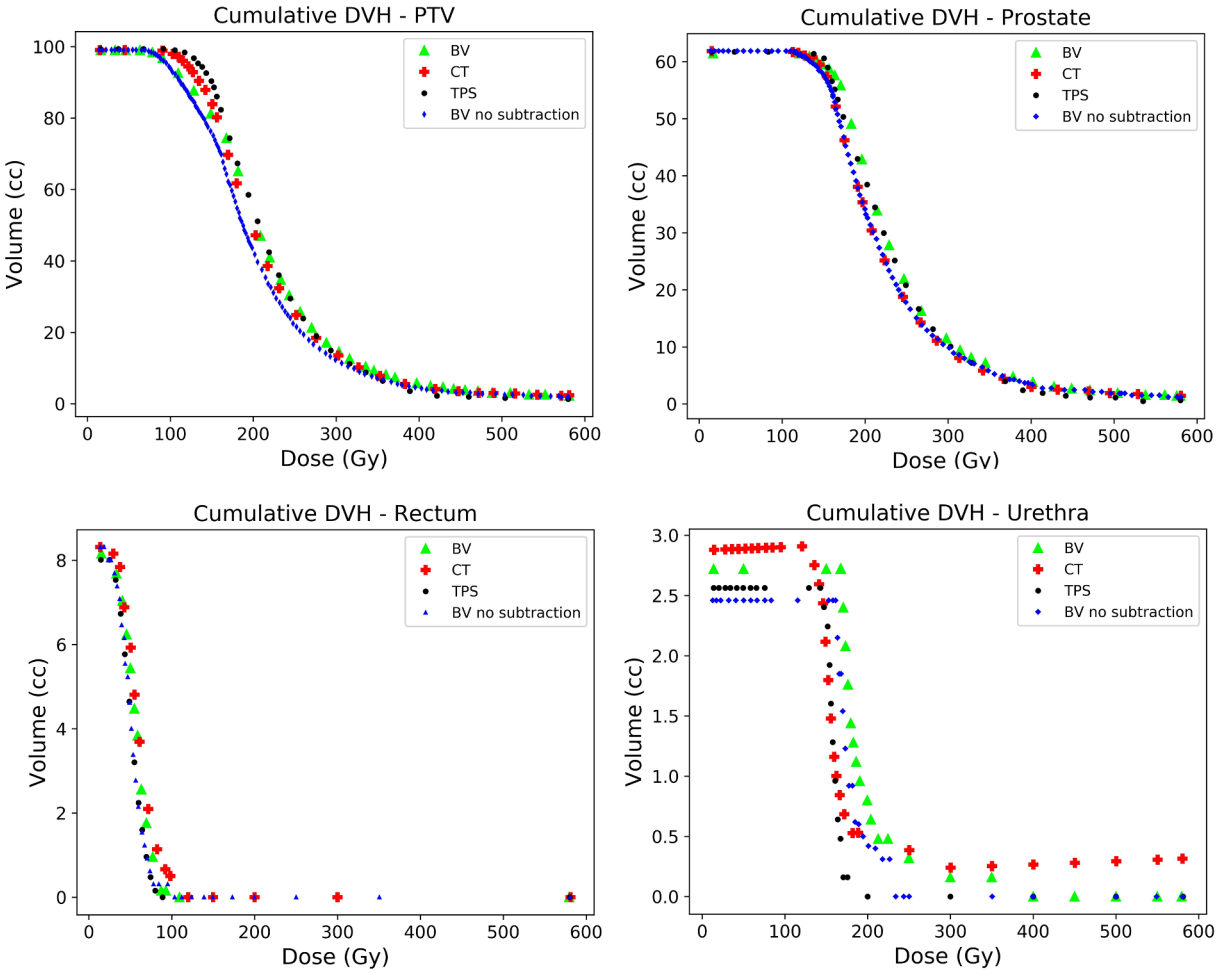

Fig. 10. Cumulative DVHs for PTV, prostate (top, left to right), rectum and urethra (bottom, left to right) comparing results for BrachyView, CT and TPS data sets.

Table 1
Percentage differences between BrachyView and CT cumulative DVH data.

Dose (Gy)	PTV % difference BV/CT	Dose (Gy)	PROSTATE % difference BV/CT	Dose (Gy)	RECTUM % difference BV/CT	Dose (Gy)	URETHRA % difference BV/CT
100	−3.84	100	0.03	15	1.81	15	−5.56
200	9.85	200	19.77	30	1.84	150	185.71
300	12.81	300	−17.03	60	16.21	170	28.52
Average difference (%)	6.27		0.92		6.62		69.56

Table 2
Percentage differences between BrachyView data without background subtraction and CT cumulative DVH data.

Dose (Gy)	PTV % difference BV/CT	Dose (Gy)	PROSTATE % difference BV/CT	Dose (Gy)	RECTUM % difference BV/CT	Dose (Gy)	URETHRA % difference BV/CT
100	−4.80	100	0.45	15	0	15	−13.19
200	−13.01	200	0.84	30	−5.64	150	83.33
300	−7.86	300	−26.27	60	−46.38	170	0
Average difference (%)	−8.38		−8.33		−17.34		23.38

anatomical direction). This is due to the lack of mechanical alignment between the probe and phantom. The main implication caused by the pinhole collimator rotation is that the reconstructed seed positions were shifted to the right-hand side of the FoV, as highlighted in Fig. 12. The effect is more evident in seeds located at large distances from the collimator, due to the triangulation (used for seed position 3D reconstruction) algorithms sensitivity to the inverse of the magnification factor (where this is given by the ratio between the source to collimator

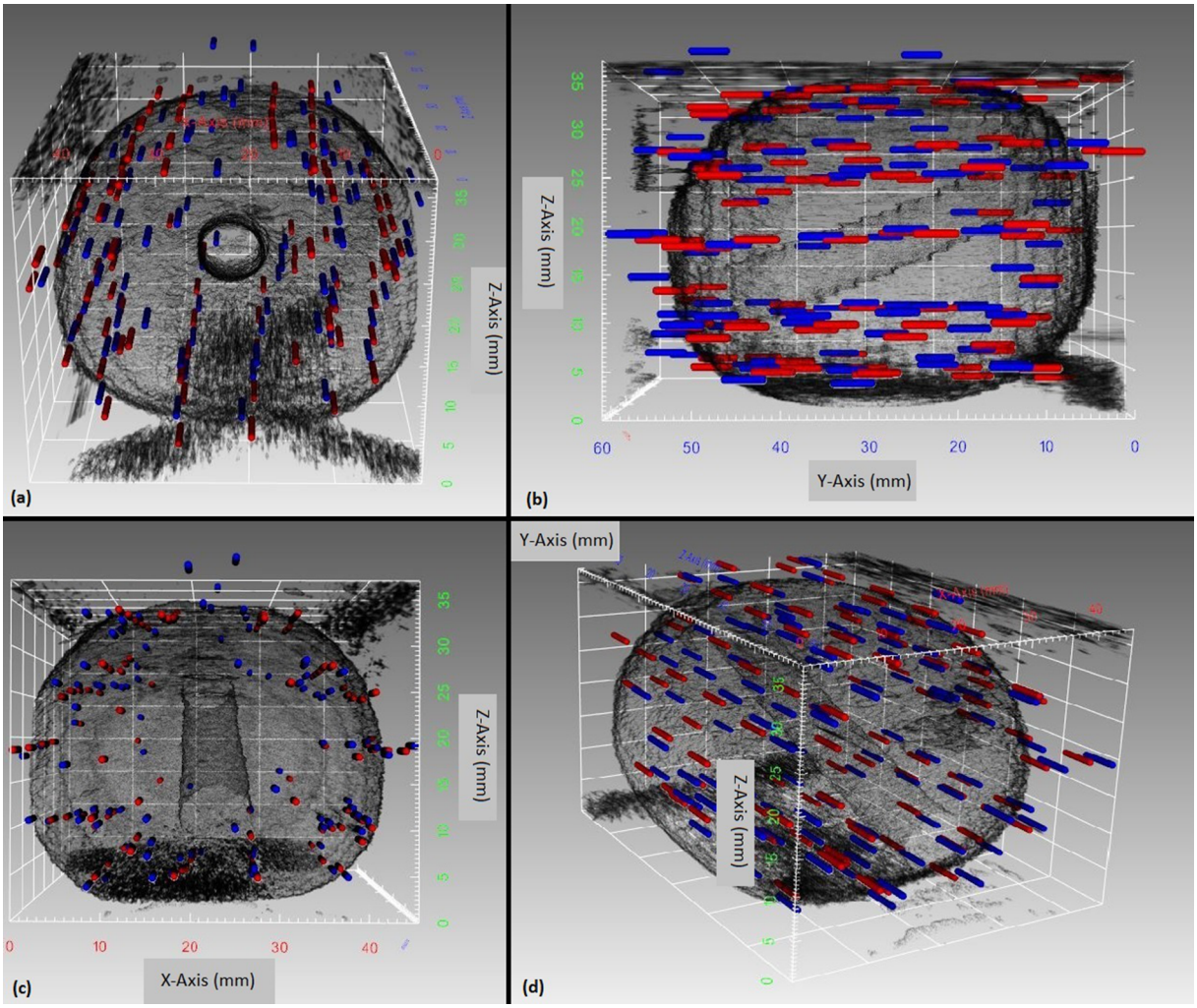

Fig. 11. 3D reconstructed gel prostate phantom with fused CT (red) and BrachyView (blue) seed positions. (For interpretation of the references to colour in this figure legend, the reader is referred to the web version of this article.)

distance (SCD) and focal length). To confirm whether the shift of the reconstructed seeds was due to a rotation of the pinhole collimator a model was derived to quantify the possible collimator rotation experienced during image acquisition using Eqs. (3) and (4). Where X_0 and Z_0 are the x and z co-ordinates as determined by the post-operative CT scan, x_1 is the x co-ordinate as reconstructed by the BrachyView system, θ is the angle required to transform the shifted co-ordinates to the nominal position and α is the angle of rotation of the probe. By iteratively computing the θ required to transform each seed back to its' nominal post-operative CT position, it was possible to determine the average angular rotation experienced by the pinhole collimator during the acquisition process.

$$x_0 = x_1 \times \frac{sin\theta}{sin(\alpha - \theta)} \tag{3}$$

$$\theta = tan^{-1}\left(\frac{X_0}{Z_0}\right) \tag{4}$$

The transformation was applied to each individual BrachyView reconstructed position along the x-axis resulting in 98% of seeds falling within 2 mm of their nominal positions. Calculation of the average α value required to transform the BrachyView data gave an estimate of the collimator rotation of 7.3°, with angles ranging from 0.07° to 28.23°, as shown in Fig. 13.

These results demonstrate that even small rotations due to mechanical misalignment of the system can result in large discrepancies in reconstructed positions. A proposed solution to mitigate the error introduced by the rotation of the pinhole collimator would be to design and fabricate a mechanical alignment system that is able to rigidly anchor the BrachyView probe to the brachytherapy stepper. One concept that could be trialled is to design a 3D printed replica of an ultrasound probe that is able to be locked into the brachytherapy stepper, just as the true ultrasound probe would be, and the BrachyView probe rigidly anchored to the end.

Average discrepancies between BrachyView positions and the CT dataset, were found to be 2.40 mm, 1.35 mm and 1.21 mm in the x, y and z axes, respectively. The differences between CT and BrachyView data are within the theoretical estimations for positional errors utilising the current method and collimator design, as outlined by M. Petasecca et al. [21]. These estimates are calculated to be 6.78 mm for x and y directions and 4.04 mm in the z-direction.

Another aspect which must be improved is the current reconstruction software architecture, which relies on user identification of newly implanted seeds and CoM for reconstruction. When baseline subtraction is not applied, seed projections belonging to implanted seeds in close proximity to high count projections are masked. This reduces the capability to identify the current later seeds and their CoM, resulting in an 8.2% reduction in the detection rate of the system. This also impacted the overall reconstruction accuracy when compared to data reconstructed with baseline subtraction implemented, resulting in a decreased accuracy of 11.5% when compared to reconstruction results

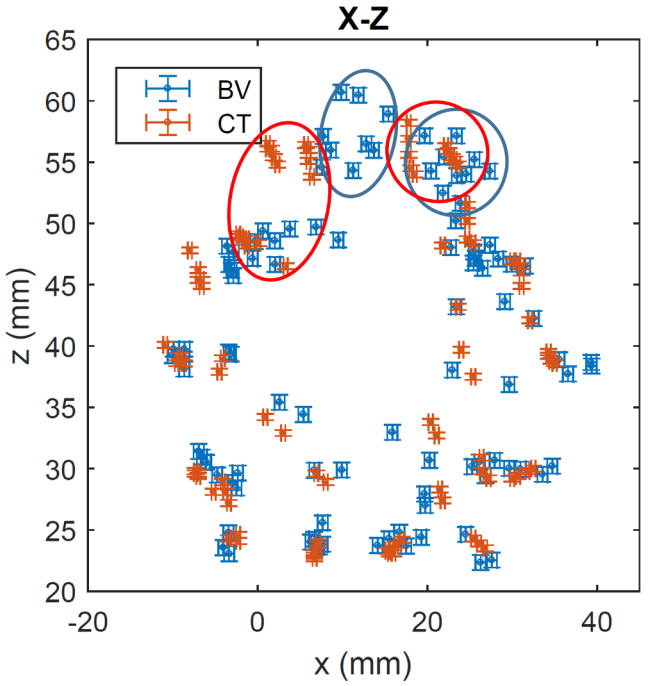

Fig. 12. X-Z reference frame 2D scatter plot showing that with increasing Z a shift effecting the X reference frame greatly increases. Resulting in a more noticeable shift in the BrachyView reconstructed positions (blue clusters), compared to the reconstructed CT positions (red clusters). (For interpretation of the references to colour in this figure legend, the reader is referred to the web version of this article.)

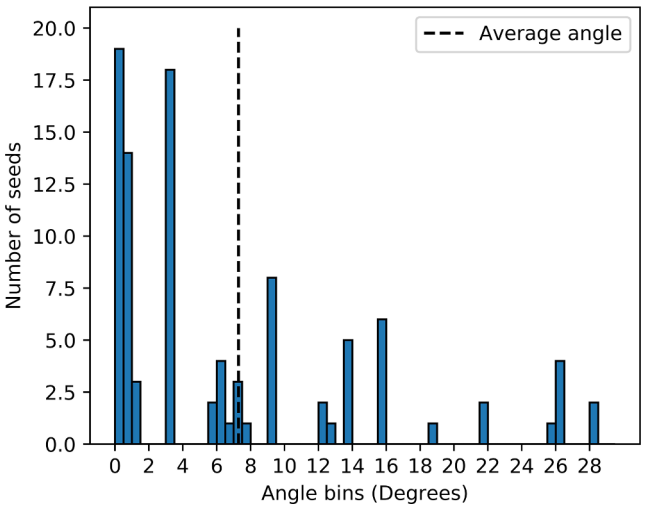

Fig. 13. Angular rotations experienced by the pinhole collimator, calculated for each seed. The dotted line represents the average rotation.

obtained with baseline subtracted data. These results clearly show the necessity for the application of a baseline subtraction algorithm, specifically for cases with large numbers of seeds. Without it, seed detection and reconstruction accuracy for the system are greatly deminished, the system would not be deemed appropriate for use with seed numbers above 30 and therefore it would not be appropriate for clinical use.

The user is also tasked with identifying the ground truth seed positions from the CT dataset, which is limited by the resolution at which the scan was performed. This study utilised a protocol with a 1 mm slice resolution with 0.5 mm overlap, limiting the accuracy of determining each seeds CoM. Implementation of a higher resolution scan could improve the accuracy, however, the settings utilised are of a higher resolution than those currently recommended for imaging of prostate implants (2–3 mm slice thickness), as outlined by AAPM Task Group 137 [11].

During implantation and subsequent imaging, it was noted that the needles being implanted were not following the specific needle implant order outlined in the VariSeed TPS documentation. This error was picked up by the BrachyView system by assessing the images immediately during the implantation. Verification of the number of seeds within a selected needle, along with its implantation location is critical in ensuring the dose distribution replicates the treatment plan. It has been shown that if the incorrect needle has been implanted, containing a different number of seeds in respect to the plan, it can produce a significant shift in the dose distribution and hence the patients' quality of treatment [8]. BrachyView has shown it can provide the means to verify needle placement and loading intraoperatively, allowing for real-time adjustment to account for errors such as miss loading of a needle and incorrect needle positioning if they were to arise.

The D90 and V100 values are used for the assessment of implant quality and hence it is critical for these values to be accurate when utilizing the BrachyView reconstructed positions. The larger discrepancy between D90 values, compared to the V100 discrepancy are caused by the presence of higher dose gradients due to the relatively sparse distribution of the seeds in the urethra and surrounding area [27], making it more sensitive to errors caused by the misalignment of the BrachyView probe. The cumulative DVH were also calculated for each dataset for the PTV, prostate, urethra and rectum, as shown in Fig. 10. The over estimation of the dose with the BrachyView data was caused due to the sparse placement of seeds close to the urethra. This resulted in a much lower seed density in this area. As previously presented by Dawson et al., with a much smaller number of seeds positioning errors become much more critical in terms of the dose distribution, with errors as little as 2 mm resulting in an underdose with I-125 of 8% and an overdose of 12% [8]. Hence the average 3D discrepancy between the CT and BrachyView of 3.28 mm ultimately results in large variations in the dose distributions for the organs at risk. A mechanical alignment system to align the BrachyView and TRUS systems will greatly improve the overall reconstruction accuracy, leading to improvements in the accuracy of the dosimetry. Without the application of the baseline subtraction algorithm this resulted in a reduction of 7.6% and 2.1% for the D90 and V100 values, respectively. With D90 and V100 being utilised to assess the quality of the implant it is very important for these values to be an accurate representation of the implant. Increased percentage differences between the BrachyView data without baseline subtraction and CT CDVH values are present, the main reason for this dosimetric variance is due to the loss of ability to reconstruct all 98 seeds, as well as a decrease in reconstruction accuracy. With the application of the baseline subtraction algorithm this resulted in improved accuracy to match the CT determined values, however, as discussed this overall dosimetric accuracy is reduced due to the positional inaccuracy noted.

It must also be noted that previous studies with the probe have utilised optimal plans to test the reconstruction capabilities of the system, where there were far fewer seeds implanted at closer distances from the detector's collimator. By contrast, this study was performed on a clinical plan that would be appropriate for a patient [28], with 98 seeds implanted at a distance up to 60 mm from the collimator, hence presenting the capabilities and robustness of the system to reconstruct a larger number of seeds in a real treatment scenario.

5. Conclusion

The BrachyView system was able to reconstruct 91.8% of implanted seeds, with an average overall discrepancy of 3.65 mm without the application of the baseline subtraction algorithm, however, with the baseline subtraction algorithm applied to the data the detection rate was improved to 100% and an increase of 11.5% in seed reconstruction

accuracy was noted. Variations in D90 and V100 values of 9% and 0.4%, respectively were found. For the system to be translated into a clinical setting it has been shown that the baseline subtraction algorithm is an integral part within the current software architecture to provide the means for high detection rates and positional accuracy. A mechanical alignment system and a seed segmentation algorithm that can automatically detect and register the CoM of each newly implanted seed in real time will also be needed. The BrachyView system can be an effective tool for intraoperative dosimetry for LDR prostate brachytherapy treatments.

References

[1] Australian Government Cancer Statistics, Prostate cancer statistics.http://prostate-cancer.canceraustralia.gov.au/statistics; 2017.

[2] Polo A. Image fusion techniques in permanent seed implantation. J Contemp Brachyther 2010;2(3):98–106.

[3] Lagerburg V, Moerland MA, Lagendijk JJ, et al. Measurement of prostate rotation during insertion of needles for brachytherapy. Radiother Oncol 2005;77(3):318–23.

[4] Yamada Y, Potters L, Zaider M, et al. Impact of intraoperative edema during transperineal permanent prostate brachytherapy on computer-optimized and pre-implant planning techniques. Am J Clin Oncol 2003;26(5):130–5.

[5] Podder T, Clark D, Sherman J, et al. In-vivo motion and force measurement of surgical needle intervention during prostate brachytherapy. Med Phys 2006;33(8):2915–22.

[6] Sadjadi H, Hashtrudi-Zaad K, Fichtinger G. Needle deflection estimation: prostate brachytherapy phantom experiments. Int J Comput Assisted Radiol Surg 2014;9(6):921–9.

[7] Badiozamani KR, Wallner K, Sutlief S, et al. Anticipating prostatic volume changes due to prostate brachytherapy. Rad Oncol Invest 1999;7(6):360–4.

[8] Dawson JE, Wu T, Roy T, et al. Dose effects of seeds placement deviations from pre-planned positions in ultrasound guided prostate implants. Radiother Oncol 1994;32:268–70.

[9] Bues M, Holupka EJ, Meskell P, et al. Effect of random seed placement error in permanent transperineal prostate seed implant. Radiother Oncol 2006;79(1):70–4.

[10] Alfredo Polo JV, Salembier Carl, Hoskin P. Review of intraoperative imaging and planning techniques in permanent seed prostate brachytherapy. Radiother Oncol 2010;94(1):12–23.

[11] Nath R, Bice WS, Butler WM, et al. Aapm recommendations on dose prescription and reporting methods for permanent interstitial brachytherapy for prostate cancer: report of task group 137. Med Phys 2009;36(11):5310–22.

[12] Sugawara A, Nakashima J, Kunieda E, et al. Incidence of seed migration to the chest, abdomen, and pelvis after transperineal interstitial prostate brachytherapy with loose 125i seeds. Rad Oncol 2011;6(1):130.

[13] Dehghan E, Moradi M, Wen X, et al. Prostate implant reconstruction from c-arm images with motion-compensated tomosynthesis. Med Phys 2011;38(10):5290–302.

[14] Zelefsky MJ, Worman M, Cohen GN, et al. Real-time intraoperative computed tomography assessment of quality of permanent interstitial seed implantation for prostate cancer. Urology 2010;76(5):1138–42.

[15] Zelefsky MJ, Cohen GN, Taggar AS, et al. Real-time intraoperative evaluation of implant quality and dose correction during prostate brachytherapy consistently improves target coverage using a novel image fusion and optimization program. Prac Rad Oncol 2017;7(5):319–24.

[16] Racine E, Hautvast G, Binnekamp D, et al. Real time electromagnetic seed drop detection for permanent implants brachytherapy: technology overview and performance assessment. Med Phys 2016;43(12):6217–25. Exported fromhttps://app.dimensions.ai on 2019/02/07.

[17] Dehghan E, Bharat S, Kung C, et al. Em enhanced us based seed detection for prostate brachytherapy. Med Phys 2018;45(6):2357–68. Exported fromhttps://app.dimensions.ai on 2019/02/07.

[18] Nath R, Anderson LL, Luxton G. et al, Dosimetry of interstitial brachytherapy sources: recommendations of the aapm radiation therapy committee task group no. 43. Med Phys 1995;22(2):209–34.

[19] Ravindran Paul B, Lewis C, Van Dyk J. Intra-operative dosimetru of trans-rectal ultrasound guided I-125 prostate implants using c-arm fluroscopic images. J Med Phys 2006;31(2):61–6.

[20] Alnaghy S, Cutajar DL, Loo KJ, et al. Brachyview: combining trans-rectal ultrasound 3d imaging and position reconstruction of ldr seeds in a prostate gel phantom. Physica Med 2017;34:55–64.

[21] Petasecca M, Loo KJ, Safavi-Naeini M. Brachyview: proof-of-principle of a novel in-body gamma camera for low dose-rate prostate brachytherapy. Med Phys 2013;40(4):041709. 041709–n/a.

[22] Han Z, Safavi-Naeini M, Alnaghy S, et al. Radiation dose enhancement at tissue-tungsten interfaces in hdr brachytherapy. Phys Med Biol 2014;59(21):6659.

[23] Loo KJ, Jakubek J, Zemlicka J, et al. Brachyview: feasibility study into the application of timepix detectors for soft tissue thickness imagining in prostate brachytherapy treatment. Rad Meas 2014;71:329–32.

[24] Brennen T, Cutajar DL, Alnaghy S, et al. Brachyview: verification of ldr patient plans – hardware optimisation. J Phys: Conf Ser 2019;1154(1).

[25] C.I.R.S.I. (CIRS) Ultrasound prostate training phantom.http://www.circinc.com/.

[26] Yu Y, Anderson LL, Li Z, et al. Permanent prostate seed implant brachytherapy: report of the american association of physicists in medicine task group no. 64. Med Phys 1999;26(10):2054–76.

[27] Georgios Koukourakis VA, Kelekis Nikolaos, Kouloulias V. Kouloulias, Brachytherapy for prostate cancer: a systematic review. Adv Urol 2009;2009:327945.

[28] Prostate Cancer Foundation of Australia. Understanding brachytherapy for prostate cancer.http://www.prostate.org.au/media/468677/understanding-brachytherapy.pdf; 2014.